0026-895X/06/7004-1194–1203$20.00
MOLECULAR PHARMACOLOGY
Copyright © 2006 The American Society for Pharmacology and Experimental Therapeutics
Mol Pharmacol 70:1194–1203, 2006

Vol. 70, No. 4
25643/3139514
Printed in U.S.A.

The Bioreduction of a Series of Benzoquinone Ansamycins by NAD(P)H:Quinone Oxidoreductase 1 to More Potent Heat Shock Protein 90 Inhibitors, the Hydroquinone Ansamycins[S]

Wenchang Guo, Philip Reigan, David Siegel, Joseph Zirrolli, Daniel Gustafson, and David Ross

Department of Pharmaceutical Sciences, School of Pharmacy and Cancer Center, University of Colorado Health Sciences Center, Denver, Colorado

Received April 12, 2006; accepted July 6, 2006

ABSTRACT

We have previously evaluated the role of NAD(P)H:quinone oxidoreductase 1 (NQO1) in the bioreductive metabolism of 17-(allylamino)-demethoxygeldanamycin (17AAG) to the corresponding hydroquinone, a more potent 90-kDa heat shock protein (Hsp90) inhibitor. Here, we report an extensive study with a series of benzoquinone ansamycins, which includes gel-danamycin, 17-(amino)-17-demethoxygeldanamycin, and 17-demethoxy-17-[[2-(dimethylamino)ethyl]amino]-geldanamycin. The reduction of these benzoquinone ansamycins by recombinant human NQO1 to the corresponding hydroquinone ansamycins was monitored by high-performance liquid chromatography (HPLC) and confirmed by liquid chromatography/mass spectrometry. Inhibition of purified yeast Hsp90 ATPase activity was augmented in the presence of NQO1 and abrogated by 5-methoxy-1,2-dimethyl-3-[(4-nitrophenoxy)methyl-]indole-4,7-dione (ES936), a mechanism-based inhibitor of NQO1, showing that the hydroquinone ansamycins were more potent Hsp90 inhibitors than their parent quinones. An isogenic pair of human breast cancer cell lines, MDA468 and MDA468/NQ16, differing in expression of NQO1, was used, and HPLC analysis showed that hydroquinone ansamycins were formed by the MDA468/NQ16 cells, which could be prevented by ES936 pretreatment. The MDA468/NQ16 cells were more sensitive to growth inhibition after treatment with the benzoquinone ansamycins compared with the MDA468 cells; this increased sensitivity could be reduced by ES936 pretreatment. The increased duration of benzoquinone ansamycin exposure showed increased potency and -fold inhibition in MDA468/NQ16 cells relative to the parental MDA468 cells. Computational-based molecular modeling studies displayed additional contacts between yeast Hsp90 and the hydroquinone ansamycins, which translated to greater interaction energies compared with the corresponding benzoquinone ansamycins. In conclusion, these studies show that the reduction of this series of benzoquinone ansamycins by NQO1 generates the corresponding hydroquinone ansamycins, which exhibit enhanced Hsp90 inhibition.

The 90-kDa heat shock protein (Hsp90) is a molecular chaperone responsible for the ATP-dependent folding, stability, and function of a number of "client" proteins that are involved in the development and progression of cancer (Maloney and Workman, 2002; Isaacs et al., 2003); these proteins include ErbB2, Raf-1, Cdk4, Met, mutant p53, telomerase hTERT, Hif-1α, and the estrogen and androgen receptors. The function of Hsp90 has been shown to be dependent on its ability to bind and hydrolyze ATP (Obermann et al., 1998; Panaretou et al., 1998; Pearl and Prodromou, 2001), and competitive inhibition of ATP binding by the natural product geldanamycin (GM), a benzoquinone ansamycin antibiotic isolated from *Streptomyces hygroscopicus*, leads to the degradation of the client proteins by the ubiquitin-proteosome pathway (Whitesell et al., 1994; Schulte et al., 1995; An et al., 1997), resulting in cell cycle arrest, differentiation, and apoptosis (Hostein et al., 2001; Munster et al., 2001). Therefore,

This work was supported by National Institutes of Health grant R01-CA51210.

W.G. and P.R. contributed equally to this work.

Article, publication date, and citation information can be found at http://molpharm.aspetjournals.org.
doi:10.1124/mol.106.025643.

[S] The online version of this article (available at http://molpharm.aspetjournals.org) contains supplemental material.

ABBREVIATIONS: Hsp90, heat shock protein 90; GM, geldanamycin; 17AAG, 17-(allylamino)-17-demethoxygeldanamycin; 17DMAG, 17-demthoxy-17-[[2-(dimethylamino)ethyl]amino]-geldanamycin; 17AG, 17-(amino)-17-demethoxygeldanamycin; NQO1, NAD(P)H:quinone oxidoreductase; $17AAGH_2$, 17-(allylamino)-17-demethoxygeldanamycin hydroquinone; ES936, 5-methoxy-1,2-dimethyl-3-[(4-nitrophenoxy)methyl-]indole-4,7-dione; 17AEP-GA, 17-demethoxy-17-[[2-(pyrrolidin-1-yl)ethyl]amino]-geldanamycin; DCPIP, 2,6-dichlorophenol-indophenol; MTT, 3-(4,5-dimethylthiazol-2-yl)-2,5-diphenyltetrazolium bromide; BSA, bovine serum albumin; rhNQO1, recombinant human NQO1; HPLC, high-performance liquid chromatography; LC/MS, liquid chromatography/mass spectrometry; DMSO, dimethyl sulfoxide.

Hsp90 is an attractive cancer drug target in that it has the potential for simultaneous disruption of multiple oncogenic signaling proteins (Csermely et al., 1998; Adams and Elliott, 2000; Richter and Buchner, 2001; Goetz et al., 2003). Furthermore, studies have revealed that the benzoquinone ansamycin Hsp90 inhibitors accumulate in tumor cells more efficiently than in normal tissue, leading to high differential selectivities (Chiosis et al., 2003). In addition, immunoprecipitation studies have shown that Hsp90 from tumor cells has an enhanced affinity for N-terminal ligands, resulting in increased ATPase activity and an increase in sensitivity to benzoquinone ansamycins, than Hsp90 in normal cells (Kamal et al., 2003).

GM, the prototypical benzoquinone ansamycin Hsp90 inhibitor, has poor aqueous solubility and displays hepatotoxicity (Supko et al., 1995), and to overcome these undesirable properties, a number of GM analogs of the benzoquinone ansamycin class have been developed, which differ only in their 17-substituent. These include 17-(allylamino)-17-demethoxygeldanamycin (17AAG), which has shown evidence of biological and clinical activity although it has poor solubility and potential toxicity, and the more water-soluble 17-demethoxy-17-[[2-(dimethylamino)ethyl]amino]-geldanamycin (17DMAG); both are currently in clinical trials (Banerji et al., 2005; Goetz et al., 2005; Smith et al., 2005). The benzoquinone ansamycins are extensively metabolized in vivo, and the 17-position of 17AAG and 17DMAG is prone to dealkylation by cytochrome P450 to generate the benzoquinone ansamycin and Hsp90 inhibitor 17-(amino)-17-demethoxygeldanamycin (17AG) (Egorin et al., 1998). The redox active quinone moiety, of the benzoquinone ansamycins, is susceptible to reduction by flavin-containing reductases to the semiquinone with subsequent generation of superoxide (Dikalov et al., 2002) or hydroquinone species (Kelland et al., 1999; Guo et al., 2005), which is dependent on one- or two-electron reduction. However, these metabolic pathways could introduce further selectivity to the activation of the benzoquinone ansamycins to a more potent species, the hydroquinone ansamycin, within tumor cells, depending on the levels and type of bioreductive enzyme present.

NAD(P)H:quinone oxidoreductase (EC 1.6.99.2, NQO1, DT-diaphorase) is an obligate two electron-reducing flavin-containing enzyme that can use either NADH or NADPH as reducing cofactors and can catalyze the direct two-electron reduction of quinones to hydroquinones (Ernster, 1967). NQO1 is expressed at high levels throughout many human solid tumors, and levels are higher in many human tumor cell lines and cancer tissues (colon, stomach, pancreatic, lung, and breast) compared with the normal equivalents (Siegel et al., 1998; Siegel and Ross, 2000; Cullen et al., 2003). NQO1 has been shown to activate a number of quinone-based bioreductive cytotoxic antitumor agents, including diaziquone, mitomycin C, 3-[5-aziridinyl-3-(hydroxymethyl)-1-methyl-4,7-dioxoindol-2-yl]prop-2-enol, streptonigrin, 2,5-diaziridinyl-3-(hydroxymethyl)-6-methyl-1,4-benzoquinone, and β-lapachone, by reduction to hydroquinone species (Siegel et al., 1990a,b; Walton et al., 1991; Beall et al., 1996; Winski et al., 1998; Pink et al., 2000).

The NQO1-mediated reduction of 17AAG using purified NQO1 and the increased sensitivity of human cancer cell lines expressing NQO1 to 17AAG were originally reported by Kelland et al. (1999). We extended these studies to examine the properties of 17-(allylamino)-17-demethoxygeldanamycin hydroquinone ($17AAGH_2$) formed after reduction of 17AAG by NQO1 (Guo et al., 2005). In addition, we also used the human breast cancer cell line MDA468, deficient in NQO1 because of a genetic polymorphism, and an isogenic paired cell line MDA468/NQ16, a stably transfected clone that expressed high levels of NQO1 protein, in combination with a mechanism-based inhibitor of NQO1 [5-methoxy-1,2-dimethyl-3-[(4-nitrophenoxy)methyl]indole-4,7-dione (ES936)] to determine the effect of NQO1 on the metabolism of 17AAG in cells. Hsp90 ATPase activity assays with purified yeast and human Hsp90 showed that $17AAGH_2$ was a more potent inhibitor of Hsp90 than the parent quinone (Guo et al., 2005). Molecular modeling studies of 17AAG and $17AAGH_2$ in the nucleotide-binding pocket of the N-terminal domain of the yeast and human Hsp90 crystal structures displayed a greater number of hydrogen bond interactions with the hydroquinone, resulting in greater interaction energies (Guo et al., 2005).

Here, we have examined the reduction of a series of benzoquinone ansamycins, which include GM, 17DMAG, 17AG, and 17-demethoxy-17-[[2-(pyrrolidin-1-yl)ethyl]amino]-geldanamycin (17AEP-GA), using purified NQO1 to the corresponding hydroquinone ansamycins (Scheme 1) and the inhibition of purified yeast Hsp90 ATPase activity by this series of benzoquinone ansamycins in the presence and absence of NQO1. To confirm the bioreduction of the benzoquinone ansamycins by NQO1 in cells, we used the human breast cancer cell line MDA468 and the isogenic paired cell line MDA468/NQO1 in combination with ES936. We have also extended our molecular modeling study to examine the interactions of both the quinone and hydroquinone forms of this series of benzoquinone ansamycins in the N-terminal domain of the yeast Hsp90 crystal structure. In this article, we describe the data for this series of benzoquinone ansamycins. Where possible, we have illustrated the full data set for the series; otherwise, we have shown the data for 17DMAG and supplemented the remaining data as supporting information.

Materials and Methods

Materials. GM, 17DMAG, and 17AEP-GA were obtained from Invivogen Inc. (San Diego, CA); 17AAG and 17AG were provided by

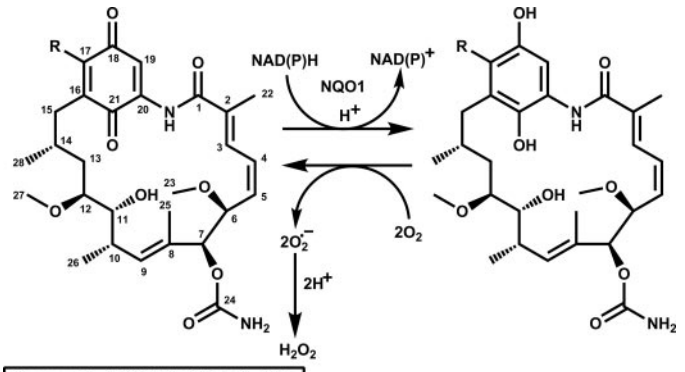

Compound	R (17-Substitutent)	MW
GM	OCH_3	560
17AAG	$NHCH_2CHCH_2$	586
17AG	NH_2	545
17DMAG	$NHCH_2CH_2N(CH_3)_2$	616
17AEP-GA	$NHCH_2CH_2NC_4H_8$	643

Scheme 1. The NQO1-mediated reduction of the benzoquinone ansamycin Hsp90 inhibitors.

the National Cancer Institute and Kosan Biosciences (Hayward, CA). 2,6-Dichlorophenol-indophenol (DCPIP), NADH, NADPH, sodium borohydride, 3-(4,5-dimethylthiazol-2-yl)-2,5-diphenyltetrazolium bromide (MTT), bovine serum albumin (BSA), β-lapachone, *N*-phenyl-1-naphthylamine, and D(−)-penicillamine were obtained from Sigma Chemical Co. (St. Louis, MO). Malachite green phosphate assay kit was obtained from BioAssay Systems Inc. (Hayward CA). Mouse anti-Hsp70 and rabbit anti-Raf-1 antibodies were obtained from Stressgen (Vancouver, BC, Canada).

ES936 was supplied by Christopher J. Moody (School of Chemistry, University of Nottingham, Nottingham, UK). Yeast Hsp90 and radicicol were obtained from Alexis (San Diego, CA). Recombinant human NQO1 (rhNQO1) was purified from *Escherichia coli* as described previously (Beall et al., 1994). The activity of rhNQO1 was 4.5 μmol of DCPIP/min/mg protein.

Cell Lines. The human breast cancer cell line MDA468 and the NQO1 stably transfected cell line MDA468/NQ16 have been described previously (Dehn et al., 2004). Cells were grown in RPMI 1640 medium containing 10% (v/v) fetal bovine serum and 1% (v/v) penicillin, streptomycin, and glutamine. MDA468 and MDA468/NQ16 cell sonicates were prepared by probe sonication in ice-cold 25 mM Tris-HCl (pH 7.4) containing 250 mM sucrose and 5 μM flavin adenine dinucleotide.

Inhibition of NQO1 by ES936. The inhibition of NQO1 by ES936, a potent mechanism-based inhibitor of NQO1, was achieved using a single dose of 100 nM ES936, which was nontoxic and resulted in >96% inhibition of NQO1 activity after 4 h in MDA468/NQ16 cells (Dehn et al., 2003).

High-Performance Liquid Chromatography and Liquid Chromatography/Mass Spectrometry Analysis. The metabolism of the benzoquinone ansamycins by NQO1 was analyzed by high-performance liquid chromatography (HPLC) on a Luna C18 5-μm, 4.6 × 250-mm reverse-phase column (Phenomenex, Torrance, CA) at room temperature. HPLC conditions were as follows: buffer A, 50 mM ammonium acetate (pH 4) containing 10 μM D(−)-penicillamine; buffer B, methanol (100%). Both buffers were continuously bubbled with argon, gradient, 30 to 90% B over 10 min, and then 90% B for 5 min (flow rate of 1 ml/min). The sample injection volume was 50 μl. Liquid chromatography/mass spectrometry (LC/MS) was performed using positive ion electrospray ionization, and the mass spectra were obtained with a PE Sciex API-3000 triple quadrupole MS (Foster City, CA) with a turbo ion spray source interfaced to a PE Sciex 200 HPLC system. Samples were chromatographed on a Luna C18 5-μm, 50 × 2-mm reverse-phase column (Phenomenex, Torrance, CA) using a gradient elution consisting of a 2-min initial hold at 20% B, followed by an increase to 80% B over 20 min at a flow rate of 200 μl/min and a sample injection volume of 20 μl. Solvent A was 10 mM ammonium acetate containing 0.1% (v/v) acetic acid (pH 4.4), and solvent B was 10 mM ammonium acetate in acetonitrile containing 0.1% (v/v) acetic acid. The mass spectrometer settings were turbo ion spray temperature of 250°C, spray needle voltage at 4500 V, declustering potential at 35 V, and focus plate at 125 V. Mass spectra were continuously recorded from 150 to 1000 atomic mass units every 3 s during the chromatographic analysis.

Hsp90 ATPase Activity Assay. Inhibition of yeast Hsp90 ATPase was measured as described previously (Rowlands et al., 2004). In brief, 2.5 μg of purified yeast Hsp90 was incubated in 100 mM Tris-HCl (pH 7.4) containing 20 mM KCl, 6 mM $MgCl_2$, 200 μM NADH, the appropriate benzoquinone ansamycin (2 and 4 μM) with or without 0.33 μg of rhNQO1, and 2 μM ES936. Reactions (25 μl) were started by the addition of 1 mM ATP and allowed to proceed at 37°C for 3 h. Reactions were then diluted with 225 μl of 100 mM Tris-HCl (pH 7.4) containing 20 mM KCl and 6 mM $MgCl_2$ mixed thoroughly, and 80 μl was transferred to each well (96-well plate) followed by 20 μl of malachite green reagent. After 10 min, trisodium citrate (83 mM) was added to stabilize the color, and plates were read at 650 nm.

Growth Inhibition Assays. Growth inhibition was measured using the MTT assay. Cells were seeded at 2×10^3 per well (96-well plate) in complete medium for 16 h. The cells were then pretreated with 100 nM ES936 or an equal amount of dimethyl sulfoxide (DMSO) for 30 min and then exposed to the appropriate benzoquinone ansamycin for 4 h, after which cells were washed free of drug and incubated in fresh medium for an additional 72 h. The increase in drug exposure time from 4 h to 72 h (continuous exposure) was performed for 17AAG and 17DMAG. Cell viability was measured by the MTT assay as described previously (Winski et al., 2001). Inhibition of rhNQO1 by ES936 was >98%.

Immunoblot Analysis. MDA468 and MDA468/NQ16 cells were grown in 100-mm plates in complete medium to ~70% confluency. For Hsp70 and Raf-1 analysis, cells were treated with DMSO or 17DMAG (50–100 nM) in 10 ml of complete medium for 24 h. After drug treatment, cells were washed in phosphate-buffered saline and then lysed by the addition of radioimmunoprecipitation assay buffer [50 mM Tris-HCl, pH 7.4, 0.5% (v/v) NP40] containing 1 Mini protease tablet (protease inhibitor mixture; Roche, Indianapolis, IN) and phosphatase inhibitors (30 mM NaF, 40 mM β-glycerophosphate, 20 mM sodium pyrophosphate, 1 mM orthovanadate, and 1 mM EGTA). Lysates were probe-sonicated (2 s) on ice and then centrifuged to remove cellular debris. Protein concentrations were determined on supernatant by the method of Lowry et al. (1951). Samples were heated to 70°C in 2× Laemmli SDS sample buffer, and proteins were separated by 12% SDS-polyacrylamide gel electrophoresis (precast minigel; Bio-Rad, Hercules CA) and then transferred to 0.4-μm polyvinylidene difluoride membranes. Membranes were blocked in 10 mM Tris-HCl, pH 8.0, 150 mM NaCl, 0.2% Tween 20, and 5% nonfat milk for a minimum of 1 h at room temperature. Anti-Hsp70 and anti-Raf antibodies were added for 1 h at room temperature. All the primary antibodies were diluted 1:1000, except actin (1:5000). Horseradish peroxidase-labeled secondary antibodies (Jackson ImmunoResearch Labs, West Grove, PA) were diluted 1:5000 and added for 30 min. Proteins were visualized using enhanced chemiluminescence detection.

Molecular Modeling of the Benzoquinone Ansamycin and Corresponding Hydroquinone Ansamycin in the Amino-Terminal Domain of the Yeast Hsp90 Crystal Structure. Molecular modeling studies were performed on a Silicon Graphics Octane 2 workstation using the InsightII software package version 2000 (Accelrys, Inc., San Diego, CA). The crystallographic coordinates for the 2.5-Å structure of the amino-terminal domain of yeast Hsp90, Protein Data Bank no. 1A4H (Prodromou et al., 1997), were obtained from the Research Collaboratory for Structural Bioinformatics Protein Data Bank. The Builder Module was used to add hydrogen to the protein structure, and the ionizable residues were corrected for physiologic pH. The benzoquinone ansamycin and the corresponding hydroquinone structures were constructed and assigned the correct atom type and bond order from the cocrystallized GM structure. Once constructed, the ligands were in turn positioned, using the coordinated system of the protein, in the nucleotide-binding domain of Hsp90; the ligand assembly was then associated with the Hsp90 protein structure. For the molecular mechanics and molecular dynamics calculations, the Discover Module was used, and the potentials and charges of the Hsp90-ligand complex were corrected using consistent valence forcefield (Dauber-Osguthorpe et al., 1988). The Hsp90-ligand complex was then minimized using the conjugate gradient method (1000 iterations). The Docking Module was used to perform the intermolecular energy calculation to determine the nonbonded interaction energy between the Hsp90 protein and the appropriate ligand. An interface 6-Å radius subset encompassing the ligand-binding domain was selected, and both van der Waals and electrostatic energies were calculated with a specified cutoff of 8 Å.

Results

The reduction of this benzoquinone ansamycin series using purified rhNQO1, with either NADH or NADPH as cofactors, generated the corresponding hydroquinone ansamycins. The incubation of the benzoquinone ansamycin of interest with rhNQO1 and NADH was monitored by HPLC analysis and resulted in the generation of the polar hydroquinone ansamycin metabolite with subsequent loss of the benzoquinone ansamycin (Fig. 1, A and B, data shown for 17DMAG; for other compounds, see supplemental data). The formation of the hydroquinone ansamycin, from the corresponding benzoquinone ansamycin, was NQO1-dependent and could be prevented by ES936, a mechanism-based inhibitor of NQO1 (Fig. 1C, data shown for 17DMAG; for other compounds, see supplemental data). In addition, the benzoquinone ansamycins could be chemically reduced using sodium borohydride to generate the hydroquinone ansamycin as previously reported (Schnur et al., 1995; Guo et al., 2005). The identification of the hydroquinone ansamycin product, from the chemical or NQO1-mediated reduction of the benzoquinone ansamycin, was confirmed by LC/MS, giving ions for GMH_2 at *m/z* 580.5 $[M+NH_4^+]^+$, $17AGH_2$ at *m/z* 548.2 $[M+H^+]^+$, $17DMAGH_2$ at *m/z* 619.3 $[M+H^+]^+$, and $17AEP\text{-}GAH_2$ at *m/z* 645.3 $[M+H^+]^+$ (Fig. 1D, data shown for 17DMAG; for other compounds, see supplemental data). All the hydroquinone ansamycins formed by the reduction of the benzoquinone ansamycins in this series were susceptible to autoxidation. The rate of autoxidation of the hydroquinone ansamycin was dependent on the substituent at the 17-position; from our studies, the GM hydroquinone from this series was the most stable (data not shown). The autoxidation of the hydroquinone ansamycin could be impeded by continuously gassing the HPLC buffers during analysis with nitrogen or argon and by the addition of a copper chelator to the HPLC buffers (see under *Materials and Methods*).

The malachite green Hsp90 ATPase activity assay has been previously used as a high-throughput screen to evaluate Hsp90 inhibition (Rowlands et al., 2004). It was used here to examine the differences in inhibitory activity of this series of benzoquinone ansamycins and their respective hydroquinones on the yeast Hsp90 ATPase reaction (Fig. 2). In these assays, purified yeast Hsp90 and ATP were incubated with the appropriate benzoquinone ansamycin (2 and 4 μM) and NADH in the presence and absence of rhNQO1 over a 3-h

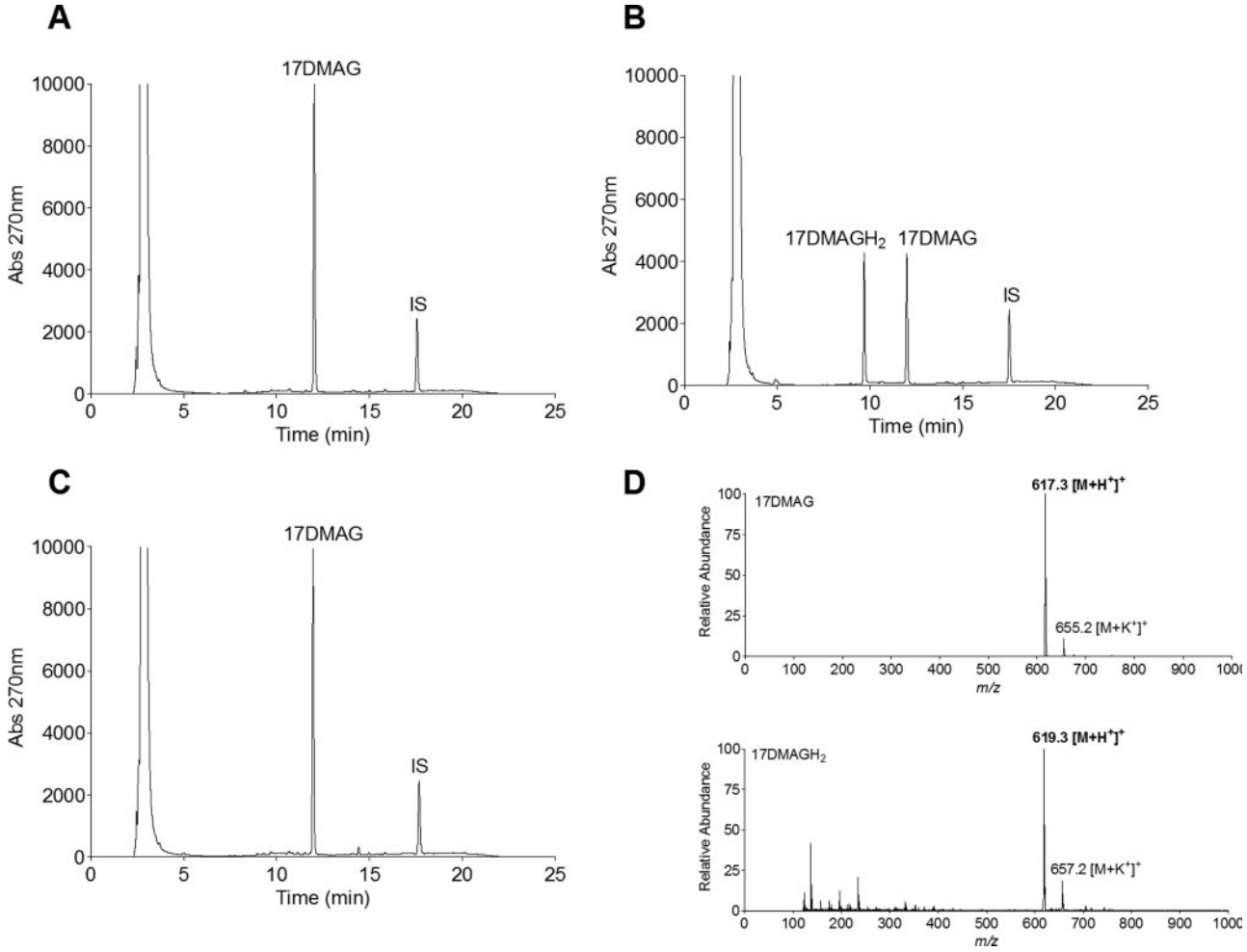

Fig. 1. HPLC and LC/MS analysis of the reduction of 17DMAG by NQO1 to $17DMAGH_2$. HPLC analysis of the rhNQO1-mediated reduction of 17DMAG (A) to $17DMAGH_2$ (B) and inhibition of this reduction by ES936 (C). A, 17DMAG and NADH; B, 17DMAG, NADH, and rhNQO1; and C, 17DMAG, NADH, rhNQO1, and ES936 (1 μM). Reaction conditions: 20 μM 17DMAG, 500 μM NADH, and 6.6 μg of rhNQO1 in 50 mM potassium phosphate buffer (pH 7.4; 1 ml) containing 1 mg/ml BSA. After 30 min, the internal standard *N*-phenyl-1-naphthylamine (10 μg/ml) was added, the sample centrifuged, and the supernatant was analyzed immediately by HPLC at 270 nm. D, LC/MS confirmed $17DMAGH_2$ as the product of NQO1-mediated reduction of 17DMAG.

period, after which reactions were terminated, and the concentration of inorganic phosphate was measured using the malachite green assay (Rowlands et al., 2004). A significant decrease in ATPase activity was observed with each of the benzoquinone ansamycins examined in the presence of NQO1 compared with that obtained for the benzoquinone ansamycins with NADH, and this could be prevented by pretreatment with ES936. At these concentrations, minimal inhibition of the Hsp90-mediated ATPase reaction was observed for 17DMAG and 17AEP-GA, which further highlighted the effect of the hydroquinone ansamycin on Hsp90 inhibition. The results from this ATPase assay showed that for this series of benzoquinone ansamycins, the hydroquinone ansamycin, generated by NQO1, was the more potent Hsp90 inhibitor.

These studies were extended to a cell-based system, and the formation of the hydroquinone ansamycins was investigated in cell sonicates prepared from the isogenic MDA468 and MDA468/NQ16 human breast cancer cell lines. These cell lines have been used previously to examine the role of NQO1 in antitumor quinone metabolism (Dehn et al., 2004), including 17AAG (Guo et al., 2005). The parental MDA468 cell line is deficient in NQO1 (<10 nmol DCPIP/min/mg) because of homozygous expression of the NQO1*2 polymorphism (Traver et al., 1997). The MDA468/NQ16 cell line was generated by the stable transfection of the parental MDA468 cell line with human NQO1, resulting in high NQO1 activity (>1800 nmol DCPIP/min/mg). The HPLC analysis of MDA468 and MDA468/NQ16 cell sonicates treated with these benzoquinone ansamycins yielded similar results to those obtained previously with 17AAG (Guo et al., 2005). The hydroquinone ansamycins were not detected in the MDA468 cell sonicates (Fig. 3A, data shown for 17DMAG; for other compounds, see supplemental data). Whereas the MDA468/NQ16 cell sonicates readily generated the hydroquinone ansamycin (Fig. 3B, data shown for 17DMAG; for other compounds, see supplemental data), which was NADH- or NADPH-dependent, and the formation of the hydroquinone could be prevented by ES936 (Fig. 3C, data shown for 17DMAG; for other compounds, see supplemental data).

The effect of growth inhibition induced by this series of benzoquinone ansamycins in the MDA468 and MDA468/NQ16 cells was determined by MTT assay. In this study, the cells were treated with the benzoquinone ansamycin for 4 h in the presence and absence of ES936 (Fig. 4, A and B, data shown for 17DMAG; for other compounds, see supplemental data). The results from these experiments showed that MDA468/NQ16 cells had increased sensitivity to the benzoquinone ansamycin (17DMAG; IC_{50}, 0.22 ± 0.05 μM) compared with parental MDA468 cells (17DMAG; IC_{50}, 2.06 ± 0.25 μM). The sensitivity to the benzoquinone ansamycin could be abrogated by pretreatment with ES936 (17DMAG + ES936; IC_{50}, 1.81 ± 0.20 μM). The natural product, nonquinone Hsp90 inhibitor, radicicol, was used as a negative control, and the growth-inhibitory effects were essentially identical in MDA468 and MDA468/NQ16 cells, reinforcing the effect of the hydroquinone on the growth inhibition observed in MDA468/NQ16 cells (Table 1). In addition, the effect of 17AAG and 17DMAG exposure time on the MDA468/NQ16 cells and the MDA468 cells was examined using the MTT cytotoxicity assay. The -fold increase in growth inhibition in MDA468/NQ16 cells relative to MDA468 cells was 12-fold with 17AAG and 9-fold with 17DMAG after a 4-h exposure. An increase in the time of exposure of cells to 17AAG or 17DMAG from 4 h to 72 h, resulted in the increase of -fold potentiation in MDA468/NQ16 cells relative to MDA468 cells to 66-fold with 17AAG (Fig. 4C) and 15-fold with 17DMAG (Fig. 4D), respectively. In agreement with cellular data, the potentiated inhibition of Hsp90 observed in MDA468/NQ16 cells resulted in increased degradation of the Hsp90 client

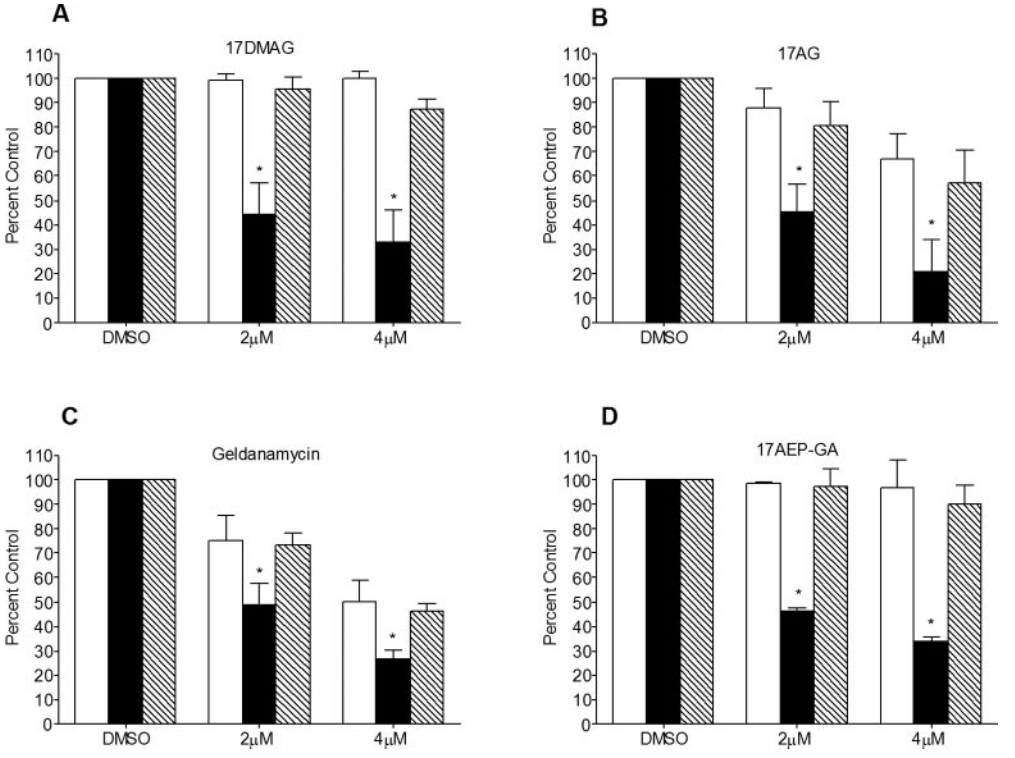

Fig. 2. Inhibition of yeast Hsp90 by the benzoquinone ansamycins. Yeast Hsp90 ATPase activity was measured in reactions with either vehicle (DMSO) or the appropriate benzoquinone ansamycin in the presence and absence of rhNQO1; the reactions were analyzed after 3 h. Phosphate concentrations were measured using the malachite green assay. Open columns, the benzoquinone ansamycin and NADH; filled columns, the benzoquinone ansamycin, NADH, and NQO1; hatched columns, the benzoquinone ansamycin, NADH, NQO1, and ES936. Columns, mean (n = 3); bars, S.D. Hsp90 ATPase activity in incubates containing the benzoquinone ansamycin, NADH, and NQO1 were statistically different from incubates containing either the benzoquinone ansamycin and NADH or the benzoquinone ansamycin, NADH, NQO1, and ES936, *, $P < 0.05$, one-way analysis of variance with Tukey for pairwise comparison.

protein, Raf-1, with a corresponding increase in Hsp70 induction (Fig. 4E, data shown for 17DMAG) relative to the parental MDA468 cells.

Molecular modeling studies of this series of benzoquinone ansamycins and their corresponding hydroquinones into the ATP-binding site of the yeast Hsp90 crystal structure revealed significant differences in the binding energies postminimization. The nonbonded interaction energy is the sum of the van der Waals and electrostatic energies, the measure of the affinity between the Hsp90 protein and the ligand investigated. In all the benzoquinone ansamycins examined, the hydroquinone had a greater nonbonded interaction energy than the parent quinone. These data support the hypothesis that the hydroquinone ansamycin is a more potent inhibitor of Hsp90. After minimization, the Hsp90-ligand complex was visualized to identify important amino acid residues in the ATP-binding domain that interact via hydrogen bonding with the ligand investigated; there was no significant change in the global conformation of Hsp90. A number of protein-ligand and through-solvent interactions lock the macrocycle of benzoquinone and the hydroquinone ansamycins in an overall conformation similar to that reported for the original yeast Hsp90-GM cocrystallized structure (Prodromou et al., 1997). The Hsp90-hydroquinone ansamycin complex revealed additional direct hydrogen-bonding interactions between the hydroquinone ansamycin and the Hsp90 protein, accounting for the greater interaction energy (Table 2, data shown for 17DMAG; for other compounds, see supplemental data), compared with the parent quinone. In the ATP-binding domain of yeast Hsp90, the C21 ketone of the benzoquinone ansamycins hydrogen bonds with the amine of Lys98, and the C18 ketone of the quinone ring system interacts with a water molecule that in turn contacts Asp40 (Fig. 5, A and C, data shown for 17DMAG; for other compounds, see supplemental data). The C21 hydroxyl of the hydroquinone ansamycins GMH_2, $17AGH_2$, and $17AEP\text{-}GAH_2$ also hydrogen bonds with the amine of Lys98, and the C18 hydroxyl of the hydroquinone ring system directly hydrogen bonds to Asp40, whereas the C21 hydroxyl of $17AAGH_2$ and $17DMAG_2$ does not interact directly with Lys98. The hydrogen atom of the C18 hydroxyl, in all the hydroquinone ansamycins examined, interacts with an oxygen atom of the carboxylate side chain of Asp40, which results in a more compact C-clamp conformation around helix-2, and in the case of the 17-amino-substituted ansamycins, the hydroquinone allows the amide of the ansa ring to interact with the backbone nitrogen of Phe124 (Fig. 5, B and D, data shown for 17DMAG; for other compounds, see supplemental data). Although no direct interactions were observed with yeast Hsp90 and the 17-substituent of the benzoquinone ansamycins or their respective hydroquinones, the side chain is orientated into solvent and does not seem to directly interfere with the binding of the ligands to the Hsp90 binding pocket.

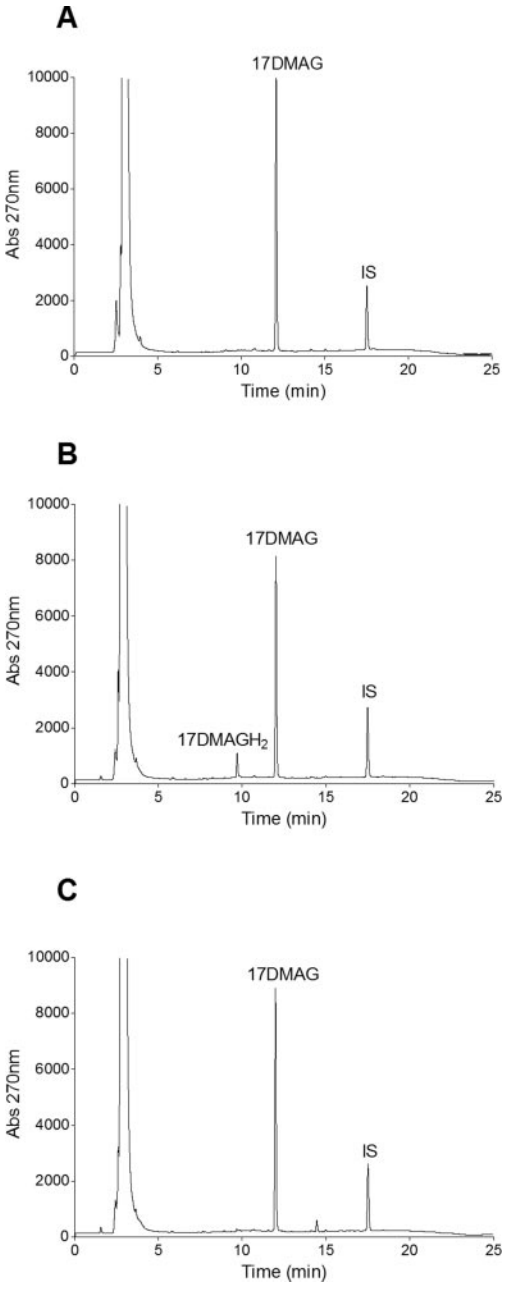

Fig. 3. HPLC analysis of $17DMAGH_2$ formation by MDA468 and MDA468/NQ16 cell sonicates. HPLC analysis confirmed the formation of $17DMAGH_2$ after reduction of 17DMAG by MDA468/NQ16 cell sonicates. A, 17DMAG, NADH, and MDA468 cell sonicates; B, 17DMAG, NADH, and MDA468/NQ16 cell sonicates; C, 17DMAG, NADH, and MDA468/NQ16 cell sonicates and ES936 (1 μM). Reaction conditions: 20 μM 17DMAG, 500 μM NADH, and 500 μg of cell sonicate in 50 mM potassium phosphate buffer (pH 7.4; 1 ml) containing 1 mg/ml BSA. After 30 min, the internal standard *N*-phenyl-1-naphthylamine (10 μg/ml) was added, the sample centrifuged, and the supernatant was analyzed immediately by HPLC at 270 nm.

Discussion

The reduction of 17AAG by NQO1 and the correlation between the cellular levels of NQO1 and sensitivity to 17AAG were first reported by Kelland et al. (1999). They also described increased inhibitory activity of GM and 17AAG in NQO1-transfected BE cells relative to NQO1-null BE parental cells and suggested that NQO1 might play a role in the cellular metabolism of these benzoquinone ansamycins (Kelland et al., 1999). We extended these studies for 17AAG by examining the purified rhNQO1-mediated reduction of 17AAG; identifying the reduction product, $17AAGH_2$, by HPLC and LC/MS; assessing the inhibition of Hsp90 ATPase activity of 17AAG and $17AAGH_2$ generated by NQO1 and abrogated by ES936; examining toxicity in isogenic MDA468 and MDA468/NQ16 cells; and investigating the interactions

of 17AAG and 17AAGH$_2$ in the ATP binding domain of Hsp90 by computational modeling (Guo et al., 2005).

In this article, we have examined a series of benzoquinone ansamycins, differing in structure only at the 17-position, to determine whether the "active" hydroquinone ansamycin hypothesis can be applied to a range of the common benzoquinone ansamycin compounds, including 17DMAG, which is currently in phase I trials in patients with metastatic, unresectable solid tumors and lymphomas. In each case, we achieved reduction of the benzoquinone ansamycin to the corresponding hydroquinone ansamycin using purified rh-NQO1; the resulting hydroquinone was identified by HPLC

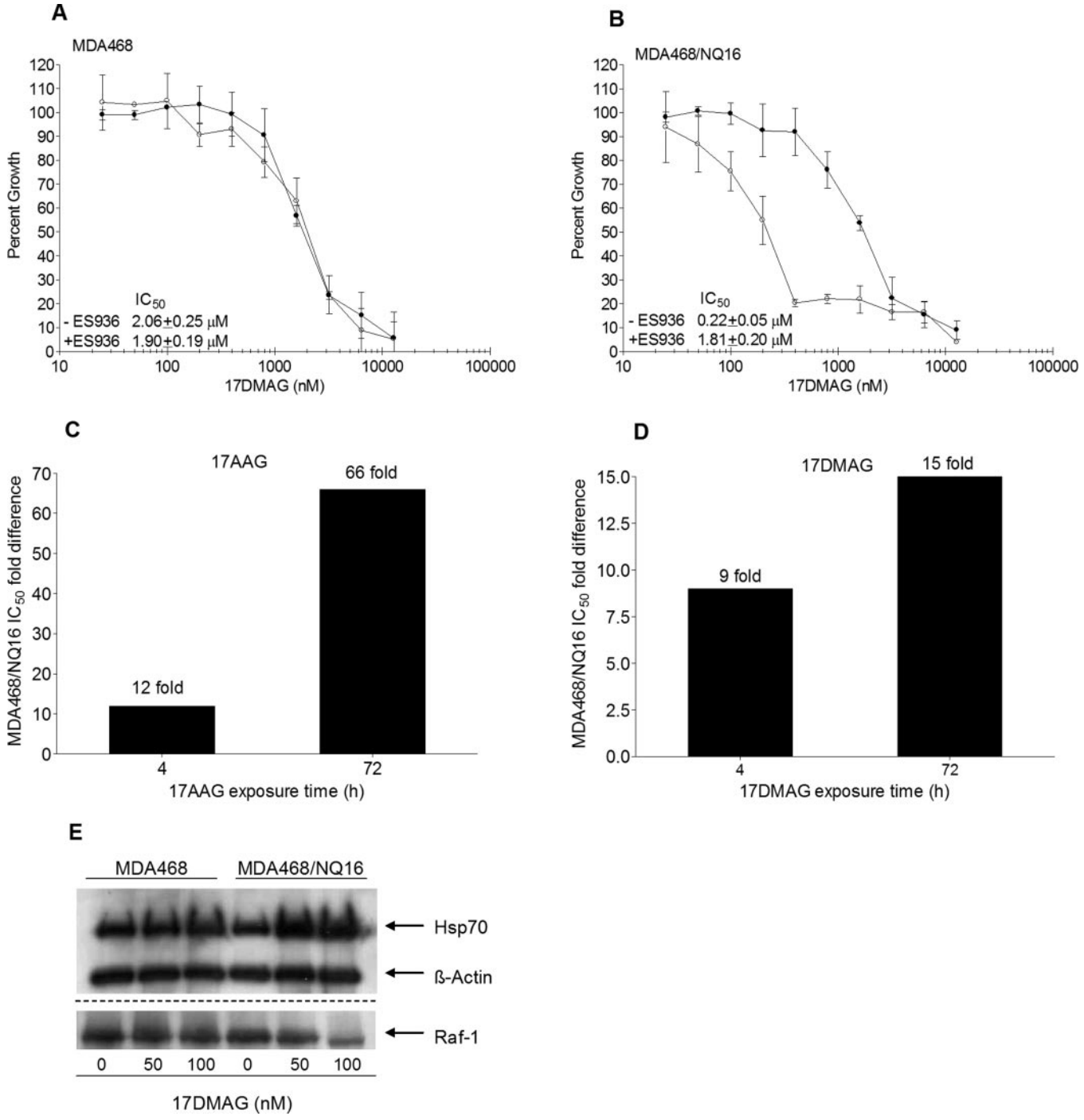

Fig. 4. Effect of 17DMAG on growth inhibition and Hsp90 client proteins in human breast cancer cells. Growth inhibition after 17DMAG treatment was measured by MTT analysis in (A) MDA468 (NQO1-null) and (B) MDA468/NQ16 (high NQO1) cell lines in the presence (filled symbols) and absence (open symbols) of ES936. Points, mean (n = 3); bars, S.D. The effect of exposure time on the -fold potentiation of (C) 17AAG and (D) 17DMAG growth inhibition in MDA468 and MDA468/NQ16 cells. IC_{50} values were measured in MDA468 and MDA468/NQ16 cells after exposure to 17AAG or 17DMAG for 4- and 72-h time periods. Data are expressed as the ratio of the IC_{50} for MDA468 cells divided by the IC_{50} for MDA468/NQ16 cells. E, the effect of 17DMAG on Hsp70 and Raf-1 protein levels. Hsp70 and Raf-1 protein levels were analyzed by immunoblot analysis after treatment of MDA468 and MDA468/NQ16 cells with 17DMAG for 24 h. Hsp70 immunoblot analysis was performed on 10 μg of whole-cell sonicate. Raf-1 immunoblot analysis was performed on 100 μg of whole-cell sonicate. Results were confirmed in duplicate experiments.

and LC/MS. To confirm that the hydroquinone ansamycins, generated by NQO1, were more potent Hsp90 inhibitors than their respective parent quinones, we used purified yeast Hsp90 to assess the ATPase activity. Indeed, as expected, the hydroquinone ansamycins were more potent inhibitors of the yeast Hsp90 ATPase reaction. The inhibition of ATPase activity by the hydroquinone ansamycins could be abrogated by use of ES936, a mechanism-based inhibitor of NQO1, confirming the role of the hydroquinone moiety in potentiating Hsp90 inhibition.

The NQO1-dependent formation of the hydroquinone ansamycins was detected by HPLC analysis in MDA468/NQ16 sonicates but not in MDA468 sonicates and could be blocked by use of ES936. Furthermore, the effect of this series of benzoquinone ansamycins on growth inhibition was increased in MDA468/NQ16 cells relative to the NQO1-deficient parental MDA468 cell line, which was consistent with previous data (Kelland et al., 1999; Guo et al., 2005). The inhibition of NQO1 with ES936 in MDA468/NQ16 cells resulted in growth inhibitory activity of the benzoquinone ansamycins to approximately those observed in the parental MDA468 cells. In addition, the nonquinone Hsp90 inhibitor, radicicol, displayed essentially the same growth inhibitory profile in both MDA468 and MDA468/NQ16 cells. These data clearly show that the increased sensitivity in cells containing elevated NQO1 levels is caused by the reduction of the benzoquinone ansamycin to the more active hydroquinone form, in concurrence with previous data (Guo et al., 2005). The increased -fold potentiation of 17AAG and 17DMAG in MDA468/NQ16 relative to MDA468 cells with increased exposure time may be a result of increased accumulation of the hydroquinone ansamycin, generated by NQO1, in cells over time, caused by the decreased lipid solubility of the hydroquinone form relative to the parent quinone. The differences in -fold potentiation between 17AAG and 17DMAG could result from the rate of NQO1-mediated reduction because 17AAG is reduced at a faster rate relative to 17DMAG (data not shown) or from the stability of the hydroquinone ansamycin formed. Therefore, the marked increase in -fold potentiation, particularly with 17AAG, could be significant with respect to antitumor effect in tumors containing high levels of NQO1. The amount of NQO1 needed to generate adequate levels of hydroquinone ansamycin sufficient for optimal growth inhibitory activity will vary from cell to cell and will depend on a variety of factors, including the reduction rate, the stability of the hydroquinone generated, and the rate of repair of any cellular damage resulting from Hsp90 inhibition.

Computational-based modeling studies of the benzoquinone ansamycins and the hydroquinone ansamycins in the nucleotide-binding domain, of the N-terminal domain, and of the yeast Hsp90 crystal structure displayed a greater number of hydrogen bond interactions between the Hsp90 protein and the hydroquinone ansamycin, resulting in increased total interaction energies compared with the parent quinone. The benzoquinone ansamycin and hydroquinone ansamycin series investigated in this study differed only in substitution at the 17-position, and in all instances, the 17-substituent pointed into solvent and did not appear to interact directly with the Hsp90 protein. The greater interaction energies of the hydroquinone ansamycins

TABLE 1
Growth inhibition effect of a series of Hsp90 inhibitors in MDA468 and MDA468/NQ16 cells following treatment (4 h)

Compound	IC_{50} (μM)				IC_{50} -Fold Difference
	MDA468	MDA468 + ES936	NQ16	NQ16 + ES936	
GM	0.063 ± 0.011	0.064 ± 0.013	0.023 ± 0.0003	0.057 ± 0.01	3
17AAG*	10.05 ± 1.07	7.34 ± 1.04	0.86 ± 0.16	7.67 ± 1.36	12
17AG	6.77 ± 0.77	6.62 ± 0.42	1.1 ± 0.11	5.61 ± 1.05	6
17DMAG	2.06 ± 0.25	1.9 ± 0.19	0.22 ± 0.05	1.81 ± 0.2	9
17AEP-GA	2.69 ± 0.08	2.68 ± 0.12	0.65 ± 0.04	2.59 ± 0.18	4
Radicicol*	3.81 ± 0.44		4.04 ± 0.35		1

* Data for 17AAG and radicicol have been reported previously (Guo et al., 2005).

TABLE 2
Total interaction energy, van der Waals, electrostatic energy, and hydrogen bonding interactions between yeast Hsp90 and 17DMAG/17DMAGH_2

Compound	E_{vdw}	E_{elect}	E_{total}	H-Bond Interaction		H-Bond Distance
				Amino Acid/Solvent	Ligand	
		kcal/mol				*Å*
17DMAG	−26.5	−27.7	−54.2	ASP-79	Carbamate NH_2	2.04
				LYS+98	Quinone C = O	1.74
				HOH400	Carbamate C = O	2.14
				HOH402	Carbamate NH_2	2.22
				HOH403	Methoxy (ansa) OCH_3	2.35
				HOH403	Carbamate R-O-$CONH_2$	2.18
				HOH405	Hydroxy (ansa) OH	2.32
				HOH407	Quinone C = O	1.65
				HOH485	Amine R-N$(CH_3)_2$	1.95
				HOH529	Amide NH	1.95
17DMAGH_2	−30.9	−28.1	−58.9	ASP-40	Hydroquinone O-H	2.00
				ASP-79	Carbamate NH_2	1.86
				PHE124	Amide C = O	2.14
				HOH400	Carbamate C = O	1.99
				HOH402	Carbamate NH_2	2.35
				HOH403	Methoxy (ansa) OCH_3	2.38
				HOH405	Hydroxy (ansa) OH	1.93
				HOH529	Amide NH	2.07

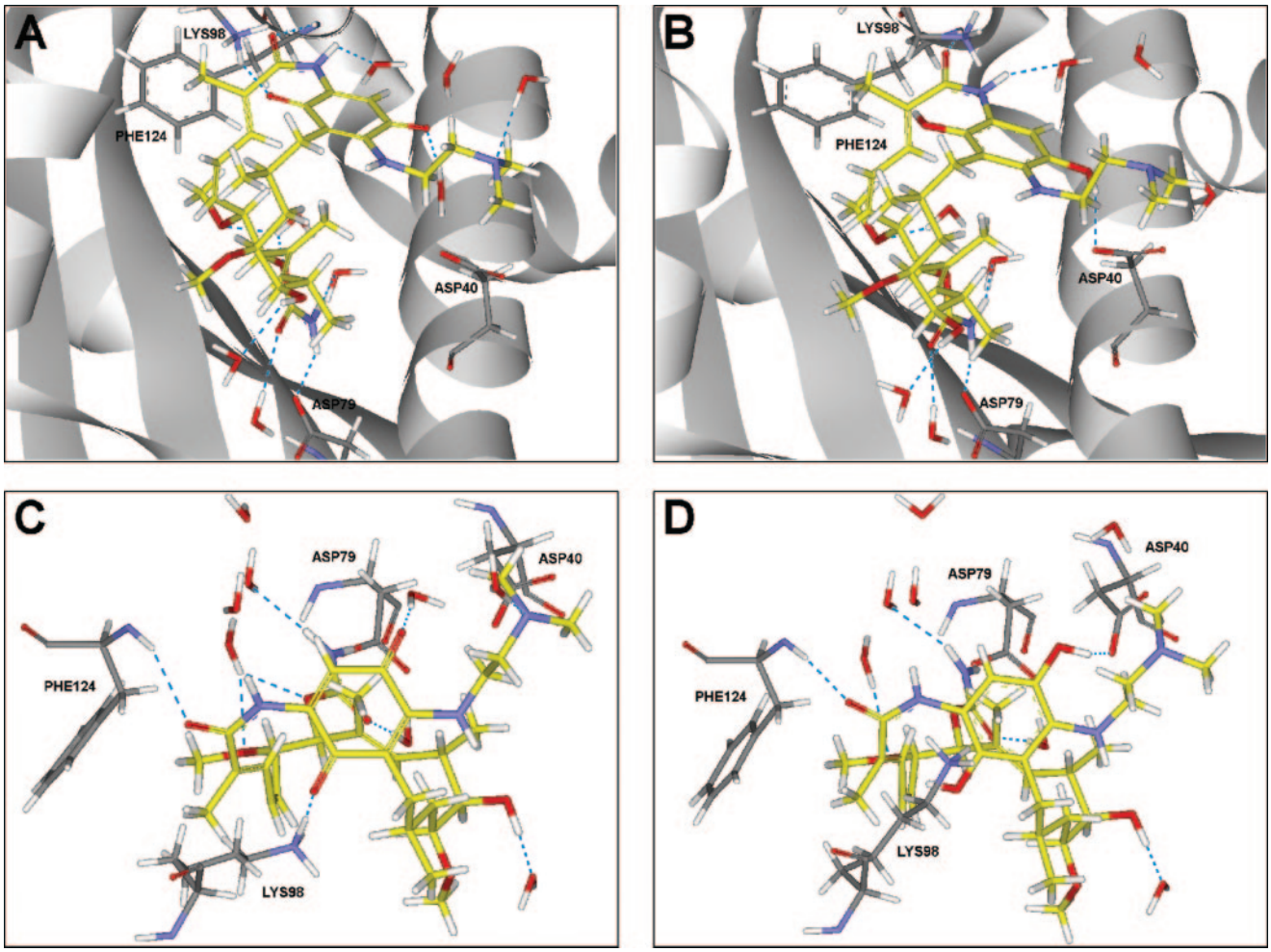

Fig. 5. Molecular modeling of the N-terminal of the yeast Hsp90–17DMAG/17DMAGH$_2$ complex. Flat ribbon representation of the yeast Hsp90 ATP-binding domain with (A) 17DMAG and (B) 17DMAGH$_2$ and stick display style representation of the key interactions with (C) 17DMAG and (D) 17DMAG; all the figures display hydrogen bond contacts (blue dashed lines) with amino acid residues and water molecules (colored by atom type, except ligand carbons atoms, which are colored yellow). The figures were constructed using Discovery Studio Viewer Professional Software (Accelrys, Inc., San Diego, CA).

can be explained by the additional direct hydrogen bond contacts with the Hsp90 protein, mainly because of the hydrogen bond donor contribution of the hydroquinone moiety, which results in a more compact C-shaped conformation that is evident from the hydrogen bonding interaction between the C18 hydroxyl and the Asp40 residue of helix-2; the strength of this interaction, as indicated by the hydrogen bond length, seems to correlate with the electrostatic contribution to the nonbonded interaction energy across this hydroquinone ansamycin series. The more compact conformation of the hydroquinone ansamycin around helix-2, the greater protein-hydroquinone ansamycin hydrogen bond contacts, and the resultant greater interaction energies for the hydroquinone ansamycins relative to the parent quinone for this series provide explanation as to why the hydroquinone ansamycins are more potent Hsp90 inhibitors.

In summary, our data show that for this series of benzoquinone ansamycins, the hydroquinone can be generated more efficiently in tumor cells containing high levels of NQO1, and that the hydroquinone form, based on target inhibition in both cell-free, cellular systems and molecular modeling studies, represents a more potent inhibitor of Hsp90. Although the parent benzoquinone ansamycins retain the ability to inhibit Hsp90 in a concentration-depen-

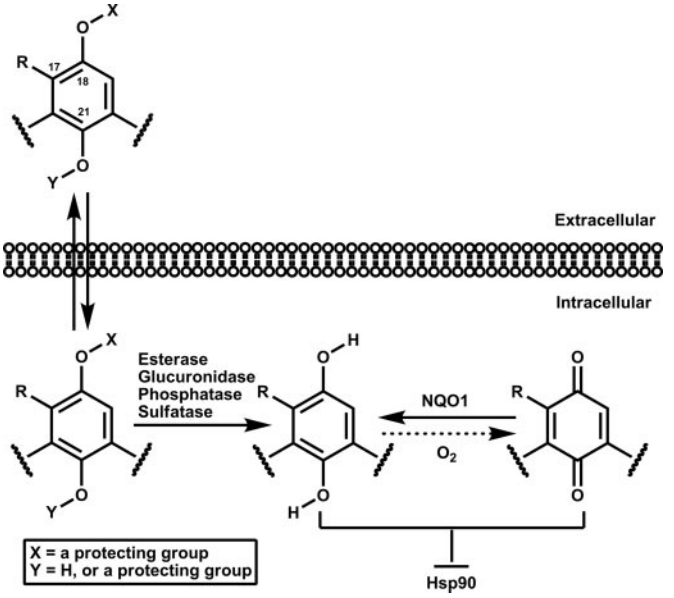

Scheme 2. A proposed model of prodrug delivery of the hydroquinone ansamycins and the maintenance of the hydroquinone form of the Hsp90 inhibitor by NQO1.

dent manner, the superior Hsp90 inhibitory potency of the hydroquinone ansamycins relative to their parent quinones has important implications for drug development.

A rational extension to this research would be to develop a prodrug approach (Scheme 2) to deliver the more potent hydroquinone ansamycin intracellularly. The generation of a series of hydroquinone ansamycin prodrugs would initially circumvent the NQO1-mediated reduction of the benzoquinone ansamycin and may additionally improve the solubility and bioavailability characteristics of the Hsp90 inhibitor. An ideal prodrug candidate would generate, via intracellular enzymatic hydrolysis, a relatively stable hydroquinone ansamycin, which is also a potent inhibitor of Hsp90 and in its quinone form is a good substrate for NQO1 to facilitate reduction back to the more potent Hsp90 inhibitor, the hydroquinone ansamycin. In addition, the hydroquinone ansamycin has increased water solubility and a decreased tendency to cross cell membranes, leading to increased accumulation of the more potent Hsp90 inhibitor, the hydroquinone ansamycin, in tumor cells containing NQO1 (Workman, 2003; Guo et al., 2005). This prodrug approach may further improve the selectivity of the Hsp90 inhibitor, in that the hydrolyzing enzyme may be specific to or more abundant in a certain tissue type.

References

Adams J and Elliott PJ (2000) New agents in cancer clinical trials. *Oncogene* **19:**6687–6692.

An WG, Schnur RC, Neckers L, and Blagosklonny MV (1997) Depletion of p185erbB2, Raf-1 and mutant p53 proteins by geldanamycin derivatives correlates with antiproliferative activity. *Cancer Chemother Pharmacol* **40:**60–64.

Banerji U, Walton M, Raynaud F, Grimshaw R, Kelland L, Valenti M, Judson I, and Workman P (2005) Pharmacokinetic-pharmacodynamic relationships for the heat shock protein 90 molecular chaperone inhibitor 17-allylamino, 17-demethoxygeldanamycin in human ovarian cancer xenograft models. *Clin Cancer Res* **11:** 7023–7032.

Beall HD, Liu Y, Siegel D, Bolton EM, Gibson NW, and Ross D (1996) Role of NAD(P)H:quinone oxidoreductase (DTdiaphorase) in cytotoxicity and induction of DNA damage by streptonigrin. *Biochem Pharmacol* **51:**645–652.

Beall HD, Mulcahy RT, Siegel D, Traver RD, Gibson NW, and Ross D (1994) Metabolism of bioreductive antitumor compounds by purified rat and human DT-diaphorases. *Cancer Res* **54:**3196–3201.

Chiosis G, Huezo H, Rosen N, Mimnaugh E, Whitesell L, and Neckers L (2003) 17AAG: low target binding affinity and potent cell activity-finding an explanation. *Mol Cancer Ther* **2:**123–129.

Csermely P, Schnaider T, Soti C, Prohaszka Z, and Nardai G (1998) The 90-kDa molecular chaperone family: structure, function, and clinical applications. A comprehensive review. *Pharmacol Ther* **79:**129–168.

Cullen JJ, Hinkhouse MM, Grady M, Gaut AW, Liu J, Zhang YP, Weydert CJ, Domann FE, and Oberley LW (2003) Dicumarol inhibition of NADPH:quinone oxidoreductase induces growth inhibition of pancreatic cancer via a superoxide mediated mechanism. *Cancer Res* **63:**5513–5520.

Dauber-Osguthorpe P, Roberts VA, Osguthorpe DJ, Wolff J, Genest M, and Hagler AT (1988) Structure and energetics of ligand binding to proteins: *Escherichia coli* dihydrofolate reductase-trimethoprim, a drug-receptor system. *Proteins* **4:**31–47.

Dehn DL, Siegel D, Swann E, Moody CJ, and Ross D (2003) Biochemical, cytotoxic and genotoxic effects of ES936, a mechanism-based inhibitor of NAD(P)H:quinone oxidoreductase 1 in cellular systems. *Mol Pharmacol* **64:**714–720.

Dehn DL, Winski SL, and Ross D (2004) Development of a new isogenic cell-xenograft system for evaluation of NAD(P)H:quinone oxidoreductase-directed antitumor quinones: evaluation of the activity of RH1. *Clin Cancer Res* **10:**3147–3155.

Dikalov S, Landmesser U, and Harrison DG (2002) Geldanamycin leads to superoxide formation by enzymatic and non-enzymatic redox cycling. Implications for studies of Hsp90 and endothelial cell nitric-oxide synthase. *J Biol Chem* **277:** 25480–25485.

Egorin MJ, Rosen DM, Wolff JH, Callery PS, Musser SM, and Eiseman JL (1998) Metabolism of 17-(allylamino)-17-demethoxygeldanamycin (NSC 330507) by murine and human hepatic preparations. *Cancer Res* **58:**2385–2396.

Ernster L (1967) DT-diaphorase. *Methods Enzymol* **10:**309–317.

Goetz MP, Toft D, Reid J, Ames M, Stensgard B, Safgren S, Adjei AA, Sloan J, Atherton P, Vasile V, et al. (2005) Phase I trial of 17-allylamino-17-demethoxygeldanamycin in patients with advanced cancer. *J Clin Oncol* **23:**1078–1087.

Goetz MP, Toft DO, Ames MM, and Erlichman C (2003) The Hsp90 chaperone complex as a novel target for cancer therapy. *Ann Oncol* **14:**1169–1176.

Guo W, Reigan P, Siegel D, Zirrolli J, Gustafson D, and Ross D (2005) Formation of 17-allylamino-demethoxygeldanamycin (17-AAG) hydroquinone by NAD(P)H: quinone oxidoreductase 1: role of 17-AAG hydroquinone in heat shock protein 90 inhibition. *Cancer Res* **65:**10006–10015.

Hostein I, Robertson D, DiStefano F, Workman P, and Clarke PA (2001) Inhibition of signal transduction by the Hsp90 inhibitor 17-allylamino-17-demethoxygeldanamycin results in cytostasis and apoptosis. *Cancer Res* **61:**4003–4009.

Isaacs JS, Xu W, and Neckers L (2003) Heat shock protein 90 as a molecular target for cancer therapeutics. *Cancer Cell* **3:**213–217.

Kamal A, Thao L, Sensintaffar J, Zhang L, Boehm MF, Fritz LC, and Burrows FJ (2003) A high-affinity conformation of Hsp90 confers tumour selectivity on Hsp90 inhibitors. *Nature (Lond)* **425:**407–410.

Kelland LR, Sharp SY, Rogers PM, Myers TG, and Workman P (1999) DT-Diaphorase expression and tumor cell sensitivity to 17-allylamino-17-demethoxygeldanamycin, an inhibitor of heat shock protein 90. *J Natl Cancer Inst* **91:**1940–1949.

Lowry OH, Rosebrough NJ, Farr AL, and Randall RJ (1951) Protein measurement with the Folin phenol reagent. *J Biol Chem* **193:**265–275.

Maloney A and Workman P (2002) HSP90 as a new therapeutic target for cancer therapy: the story unfolds. *Expert Opin Biol Ther* **2:**3–24.

Munster PN, Srethapakdi M, Moasser MM, and Rosen N (2001) Inhibition of heat shock protein 90 function by ansamycins causes the morphological and functional differentiation of breast cancer cells. *Cancer Res* **61:**2945–2952.

Obermann WM, Sondermann H, Russo AA, Pavletich NP, and Hartl FU (1998) In vivo function of Hsp90 is dependent on ATP binding and ATP hydrolysis. *J Cell Biol* **143:**901–910.

Panaretou B, Prodromou C, Roe SM, O'Brien R, Ladbury JE, Piper PW, and Pearl LH (1998) ATP binding and hydrolysis are essential to the function of the Hsp90 molecular chaperone in vivo. *EMBO (Eur Mol Biol Organ) J* **17:**4829–4836.

Pearl LH and Prodromou C (2001) Structure, function, and mechanism of the Hsp90 molecular chaperone. *Adv Protein Chem* **59:**157–186.

Pink JJ, Planchon SM, Tagliarino C, Varnes ME, Siegel D, and Boothman DA (2000) NAD(P)H:quinone oxidoreductase activity is the principal determinant of β-lapachone cytotoxicity. *J Biol Chem* **275:**5416–5424.

Prodromou C, Roe SM, O'Brien R, Ladbury JE, Piper PW, and Pearl LH (1997) Identification and structural characterization of the ATP/ADP-binding site in the Hsp90 molecular chaperone. *Cell* **90:**65–75.

Richter K and Buchner J (2001) Hsp90: chaperoning signal transduction. *J Cell Physiol* **188:**281–290.

Rowlands MG, Newbatt YM, Prodromou C, Pearl LH, Workman P, and Aherne W (2004) High-throughput screening assay for inhibitors of heat-shock protein 90 ATPase activity. *Anal Biochem* **327:**176–183.

Schnur RC, Corman ML, Gallaschun RJ, Cooper BA, Dee MF, Doty JL, Muzzi ML, Moyer JD, DiOrio CI, Barbacci EG, et al. (1995) Inhibition of the oncogene product p185erbB-2 in vitro and in vivo by geldanamycin and dihydrogeldanamycin derivatives. *J Med Chem* **38:**3806–3812.

Schulte TW, Blagosklonny MV, Ingui C, and Neckers L (1995) Disruption of the Raf-1-Hsp90 molecular complex results in destabilization of Raf-1 and loss of Raf-1-Ras association. *J Biol Chem* **270:**24585–24588.

Siegel D, Franklin WA, and Ross D (1998) Immunohistochemical detection of NAD(P)H:quinone oxidoreductase in human lung and lung tumors. *Clin Cancer Res* **4:**2065–2070.

Siegel D, Gibson NW, Preusch PC, and Ross D (1990a) Metabolism of mitomycin C by DT-diaphorase: role in mitomycin C-induced DNA damage and cytotoxicity in human colon carcinoma cells. *Cancer Res* **50:**7483–7489.

Siegel D, Gibson NW, Preusch PC, and Ross D (1990b) Metabolism of diaziquone by NAD(P)H:(quinone acceptor) oxidoreductase (DT-diaphorase): role in diaziquone induced DNA damage and cytotoxicity in human colon carcinoma cells. *Cancer Res* **50:**7293–7300.

Siegel D and Ross D (2000) Immunodetection of NAD(P)H:quinone oxidoreductase 1 (NQO1) in human tissues. *Free Radic Biol Med* **29:**246–253.

Smith V, Sausville EA, Camalier RF, Fiebig HH, and Burger AM (2005) Comparison of 17-dimethylaminoethylamino-17-demethoxy-geldanamycin (17DMAG) and 17-allylamino-17-demethoxygeldanamycin (17AAG) in vitro: effects on Hsp90 and client proteins in melanoma models. *Cancer Chemother Pharmacol* **56:**126–137.

Supko JG, Hickman RL, Grever MR, and Malspeis L (1995) Preclinical pharmacologic evaluation of geldanamycin as an antitumor agent. *Cancer Chemother Pharmacol* **36:**305–315.

Traver RD, Siegel D, Beall HD, Phillips RM, Gibson NW, Franklin WA, and Ross D (1997) Characterization of a polymorphism in NAD(P)H: quinone oxidoreductase (DT-diaphorase). *Br J Cancer* **75:**69–75.

Walton MI, Smith PJ, and Workman P (1991) The role of NAD(P)H:quinone reductase (EC 1.6.99.2, DT-diaphorase) in the reductive bioactivation of the novel indoloquinone antitumor agent EO9. *Cancer Commun* **3:**199–206.

Whitesell L, Mimnaugh EG, De Costa B, Myers CE, and Neckers LM (1994) Inhibition of heat shock protein HSP90-pp60v-src heteroprotein complex formation by benzoquinone ansamycins: essential role for stress proteins in oncogenic transformation. *Proc Natl Acad Sci USA* **91:**8324–8328.

Winski SL, Hargreaves RH, Butler J, and Ross D (1998) A new screening system for NAD(P)H:quinone oxidoreductase (NQO1)-directed antitumor quinones: identification of a new aziridinylbenzoquinone, RH1, as a NQO1-directed antitumor agent. *Clin Cancer Res* **4:**3083–3088.

Winski SL, Swann E, Hargreaves RH, Dehn DL, Butler J, Moody CJ, and Ross D (2001) Relationship between NAD(P)H:quinone oxidoreductase 1 (NQO1) levels in a series of stably transfected cell lines and susceptibility to antitumor quinones. *Biochem Pharmacol* **61:**1509–1516.

Workman P (2003) Auditing the pharmacological accounts for Hsp90 molecular chaperone inhibitors: unfolding the relationship between pharmacokinetics and pharmacodynamics. *Mol Cancer Ther* **2:**131–138.

Address correspondence to: David Ross, Department of Pharmaceutical Sciences, School of Pharmacy, University of Colorado at Denver and Health Sciences Center, C-238, 4200 East 9th Avenue, Denver, CO 80262. E-mail: david.ross@uchsc.edu